InP-Based Cylindrical Microcavity Light-Emitting Diodes

Weidong Zhou, *Student Member, IEEE*, Pallab Bhattacharya, *Fellow, IEEE*, and Omar Qasaimeh

***Abstract*—We have investigated the properties of InP-based microcavity light-emitting diodes ($\lambda = 1.6$ μm). Our objective was mainly to study the effects of lateral confinement of optical modes, which was achieved by the wet oxidation of double $In_{0.52}Al_{0.48}As$ layers. The smallest devices had a cavity radius of 0.5 μm, which becomes comparable to λ/n, where n is the effective refractive index of the photon emitting heterostructure. Two types of devices were tested: the first without any mirrors in the vertical direction, and the second with a combination of MgF/ZnSe DBR (top) and silver (bottom) to produce a low $Q \sim 35$–45. The latter type of devices exhibited higher output power and narrower spectral linewidth; otherwise, the characteristics were very similar. The output slope efficiency monotonically decreases with reduction of lateral cavity size up to ~2-μm in diameter and then is enhanced again for smaller cavity sizes. The slope efficiency of the smallest device (aperture diameter 1 μm) is almost equal to that measured for the largest devices. The maximum output power measured from the devices is 30 μW. The far-field pattern of devices with aperture radii ranging from 1.5 to 20 μm shows an angular width (FWHM) of 50°. On the other hand, devices with smaller aperture (radius ~0.5 μm) exhibit an angular width of 20°. The measured small-signal modulation bandwidth increases from ~0.45 GHz for the larger devices to 0.8 GHz for the smallest devices. Our results indicate that microcavity effects can be observed with only lateral photon confinement, making device fabrication requirements less stringent compared to surface-emitting lasers.**

***Index Terms*—Light-emitting diodes, long-wavelength emitters, microcavity, wet-oxidation.**

I. Introduction

HIGH-EFFICIENCY, reliable, and low-cost InP-based 1.55-μm light emitters will continue to play an important role in the development of long-wavelength optical fiber communication systems. Vertical-cavity surface-emitting lasers (VCSELs) are promising devices because they potentially offer efficient fiber coupling, the capability of wafer-scale fabrication and testing, 2-D arrays, large packing densities, and low-voltage operation [1]. However, the development of long-wavelength VCSELs has lagged behind the shorter wavelength (0.8–1.0 μm) GaAs-based devices, mainly due to the difficulty involved in realizing suitable epitaxial mirrors. The low index contrast existing in lattice-matched InP-based heterostructures necessitates the growth of 40–50 pairs of hi–lo index materials to form the distributed Bragg reflector (DBR) at each end of the cavity. This invariably leads to a nonplanar device structure and difficulties in processing. While other technologies are being explored [2]–[4] for long-wavelength VCSELs, an alternative approach would be to use the confinement effects of photons in a microcavity light-emitting diode (MCLED) [5]–[9].

An incoherent LED normally emits in many spontaneous modes. The light output is Lambertian and the power density is small. If, on the other hand, the recombination volume is shrunk to the order of the wavelength λ in the material, then the photon density of states is modified (develops singularities) and the emitted photons couple into the single-cavity resonance mode. The spontaneous emission rate can be greatly enhanced, accompanied by spatial coherence and increased directionality in the output. The increased spontaneous emission can lead to an enhancement in the modulation bandwidth. All these attributes make MCLEDs very attractive sources for fiber communication [6]. Additional potential advantages are high power efficiency, high fiber coupling efficiency, and low crosstalk in array applications, and simple processing accompanied by high device reliability.

Some of the effects described above have indeed been observed in resonant, or planar, Fabry–Perot microcavities [10]–[13]. These devices are generally characterized by a $n\lambda/2$ thick cavity with a photon-emitting region bounded by high reflecting mirrors ($R > 0.95$). In current technology, these mirrors are multilayer dielectric or epitaxial semiconductor DBRs. Hence, they pose the same fabrication problems as VCSELs with InP-based materials. Of more interest are the properties of microcavities in which the photon mode densities are modified primarily by *lateral* confinement [14], [15]. In principle, 3-D confinement in these devices can be obtained by incorporating mirrors in the top and bottom of the $n\lambda/2$ spacer, but this may not be necessary. In a practical device, the semiconductor-air interface should suffice. Our objective was, therefore, to study the effects of lateral confinement in cylindrical MCLEDs. Most of the work on the microcavities has been done at λ ~0.8–0.9μm [10]–[17] and very little has been reported on 1.3 and 1.55 μm MCLEDs [18]–[20]. The two device structures that are generally used to enable lateral mode confinement are etched air-post and oxide-confined, or apertured, microcavities. Surface carrier recombination dominates the characteristics of the former. The latter appears to be more promising and has been intensively investigated experimentally with the GaAs/AlGaAs material system in the context of VCSELs [21]–[24]. The properties of oxide-confined GaAs/AlGaAs MCLEDs have also been reported [25]. In the InP-based LED heterostructure, we create the confining aperture by the wet oxidation of $In_{0.52}Al_{0.48}As$, whose oxidation properties have been studied by us and applied to 1.55 μm

Manuscript received May 1, 2000; revised September 1, 2000. This work was supported by the Office of Naval Research under Grant N000 014-96-1-0024 and by the Army Research Office (MURI program) under Grant DAAG55-98-1-0288.

The authors are with the Department of Electrical Engineering and Computer Science, University of Michigan, Ann Arbor, MI 48109-2122 USA.

Publisher Item Identifier S 0018-9197(01)00389-X.

VCSELs [26], [27]. Decrease in the lateral aperture size in oxide-confined devices will result in increasing scattering loss due to phase discontinuity in the field at the abrupt index step boundary between the oxide and the unoxidized regions. It is, therefore, important to investigate the effect of aperture size on device performance.

In this paper we describe the measured characteristics of 1.6-μm InP-based oxide-apertured MCLEDs. We have investigated two types of microcavity LEDs. The lateral photon confinement in both is achieved by forming apertured cavities. In the first structure no additional mirror is formed in the vertical direction. In the second, a DBR on top and a thin-film silver reflector in the bottom, to produce a cavity with a low Q of $\sim$35–45, is incorporated to investigate the effects of such weak confinement. An InP/InAlAs/InP double-oxide confinement structure has been incorporated in the device to achieve good lateral modal confinement for the small aperture sizes. As stated before, our primary objective was to study the changes in the properties of the MCLEDs when the lateral dimension for mode confinement approaches the wavelength in the material. The device structures are described in Section II. The measured characteristics are described and analyzed in Section III. The results are summarized in Section IV.

II. Device Fabrication

A. Lateral Oxidation of $In_{0.52}Al_{0.48}As$

Lateral wet oxidation of Al-bearing compounds is usually done in a N_2 ambient saturated with water vapor, by bubbling the N_2 through a water bath held at 90°C. Oxidation is done in time periods ranging from 1 to 6 h and temperatures ranging from 300 °C to 500 °C. While it is easy to achieve a high oxidation rate in $Al_xGa_{1-x}As$ due to the high Al content $(0.9 \leq x \leq 1.0)$ in the alloys that are usually oxidized in device structures, the relatively low Al content in $In_{0.52}Al_{0.48}As$ lattice-matched to InP results in very low lateral oxidation rates [28]. The oxidation times are, therefore, long. Other materials, such as AlAsSb [29] and strain-compensated superlattice structures [30], which have higher oxidation rates, are being investigated for use with InP-based heterostructures, but there are associated problems. With the oxidation of AlAsSb, an additional layer of residual elemental Sb forms above the oxidizing layer, deforming the surrounding layer, possibly posing limitations on its use in optoelectronic devices.

We have investigated the lateral oxidation rate of $In_{0.52}Al_{0.48}As$ and have found that the alloy sandwiched between InP layers has a relatively high oxidation rate, compared to that confined between $In_{0.53}Ga_{0.47}As$ layers, due to an easier channel for As loss provides in the InP/InAlAs/InP heterostructures [26]. In this work, we have utilized the InP/InAlAs/InP heterostructure and its lateral oxidation to provide lateral-mode confinement in microcavity LEDs.

B. Microcavity Light-Emitting Diodes

The LED heterostructures were grown by metal-organic vapor phase epitaxy (MOVPE). As shown in Fig. 1(a), the devices are made with InP-based heterostructures and consist of an InGaAs bulk recombination region buried in InGaAsP

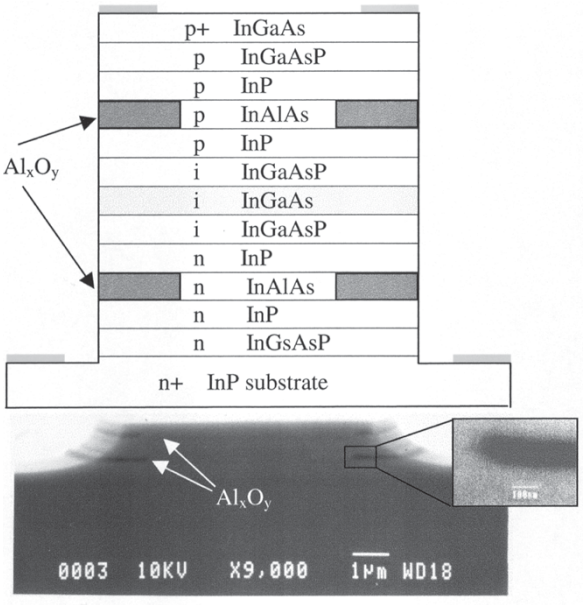

(a)

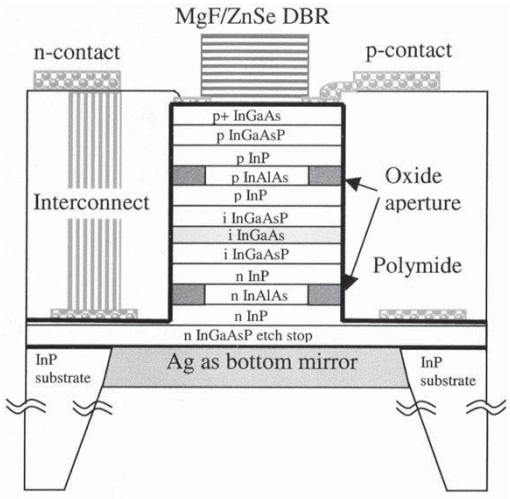

(b)

Fig. 1. (a) Heterostructure and schematic of mirror-free LEDs with a cross-sectional SEM image showing the lateral oxide confined aperture. (b) Schematic of 3-D MCLEDs with lateral oxide confinement layers, vertical silver, and DBR mirrors.

or InP spacers of thickness λ/n ($\lambda \sim 1.6$ μm). A 120-nm thick $In_{0.52}Al_{0.48}As$ layers are incorporated at both the top and bottom of the cavity, and appropriate p-type (top) and n-type (bottom) contact layers are included on both sides. Device processing starts with mesa patterning and wet etching down to the n-InP layer, as shown in Fig. 1(a), with an etch depth of 1.7 μm. The mesas have diameters ranging from 10 to 50 μm. Lateral wet oxidation of the InAlAs layer lasts for 6 h at 475 °C, which results in a lateral oxidation length of $\sim$5.5 μm. The exact oxidation length and aperture size are determined by cross-sectional scanning electron micrographs (SEMs), as shown in Fig. 1(a). No deformations of the surrounding InP and InGaAsP layers in the heterostructure were detected in a close examination of cleaved samples, as shown in the magnified SEM micrograph of Fig. 1(a). The moderate oxidation rate results in a higher quality oxide and a smaller density

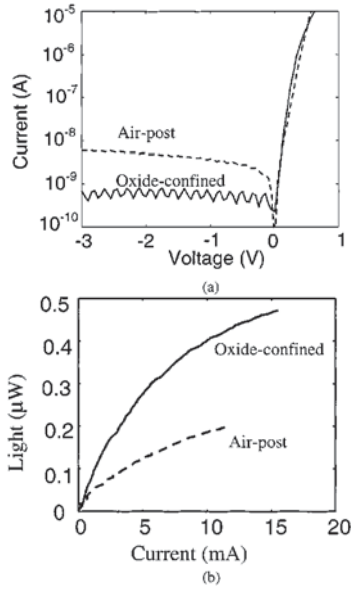

Fig. 2. (a) *I–V* and (b) *L-I* characteristics for air-post and oxide-confined devices with the same aperture size of 12 μm. Note the higher power efficiency and lower leakage current measured in the latter device.

($\sim 10^{11}$ cm^{-2}) of interface states [31], [32]. This is particularly important for devices with smaller aperture diameters. The resulting aperture, of diameters ranging from 1 to 30 μm, provides both current confinement and lateral mode confinement. Formation of n- and p-type contact metals using evaporation, photolithography and lift-off techniques, polymide planarization and Ti/Al/Ti/Au interconnect formation complete device fabrication for the mirror-free LEDs. Some of the devices were isolated at this stage for testing. Processing was continued with the rest of the devices to form the top and bottom mirrors [Fig. 1(b)]. The substrate was lapped and polished down to $\sim$90 μm, and backside holes were selectively formed in the substrate, while 100 nm of silver was evaporated onto the backside to form a backside reflector with a reflectivity of $\sim$92%. Finally, MgF/ZnSe dielectric DBRs were evaporated on top of the devices. Due to the anisotropic wet-etching characteristics of InP in HCl:acetic acid:H_3PO_4 to form the backhole, it was found desirable to orient the device along the [011] direction on the (001)-oriented wafers. Undercut produced during etching was significantly reduced in this direction. The Q of the cavity in the vertical direction is estimated to be 35–45.

From the measured current-voltage *(I–V)* characteristics, as shown in Fig. 2(a), it was observed that the reverse leakage current of the oxide-confined devices was an order of magnitude smaller than that for air-post devices of comparable lateral size. Furthermore, from the measured light-current *(L–I)* characteristics [Fig. 2(b)], it was found that the output power and slope efficiency was higher by a factor of 2 in the oxide-confined devices.

III. Device Characteristics

A. Output Power and Efficiency

The measured light-current (*L-I*) characteristics of the MCLEDs with and without top and bottom mirrors are shown

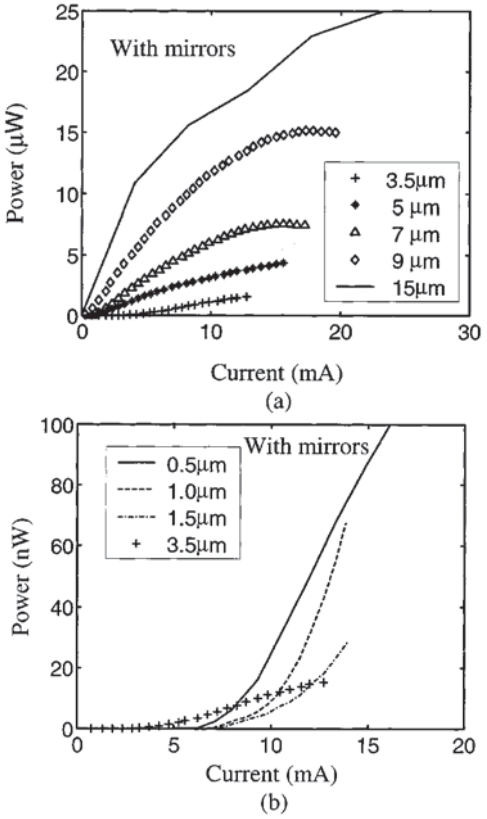

Fig. 3. *L-I* characteristics of LEDs *with* top and bottom mirrors for (a) large and (b) small aperture sizes. A distinct "turn-on" characteristic is observed for small lateral aperture sizes, as shown in (b).

in Figs. 3 and 4, respectively, for cavities of different lateral sizes (as defined by the oxide aperture). It may be noted that we have characterized devices over a large and continuous range of aperture sizes. While the larger devices show a more normal LED behavior, the smaller devices (aperture diameter less than 3 μm) show a distinct "turn-on" at low bias currents. Furthermore, the saturation behavior is also not observed in the output of these devices. The turn-on could be due to a relatively large carrier loss caused by nonradiative surface recombination. The surface-to-area ratio of the mesas increases as the device size becomes smaller. Another contributing factor is the photon loss via the radiation modes in directions other than the vertical direction of the guided modes [14]. The maximum measured output power normal to the surface is 30 μW at a bias of 30 mA for a device with an aperture size of 30 μm, with a maximum responsitivity of 2.6 mW/A, which corresponds to a slope efficiency of 0.33%. It is interesting to note that if the initial zero-output region was not present, the output characterics would resemble the ideal behavior expected of a wavelength-sized MCLED. Shown in Fig. 5 is the output slope efficiency measured for devices with and without DBR and Ag mirrors. The slope efficiency monotonically decreases with decreasing lateral aperture size and then increases again for sizes smaller than 2 μm. In fact, the efficiency for the 1-μm devices is almost as high as that for the largest devices. The distinct enhancement in the smallest devices is most likely due to an enhancement in the spontaneous emission rate, as predicted in [14] and shown later in the calculated

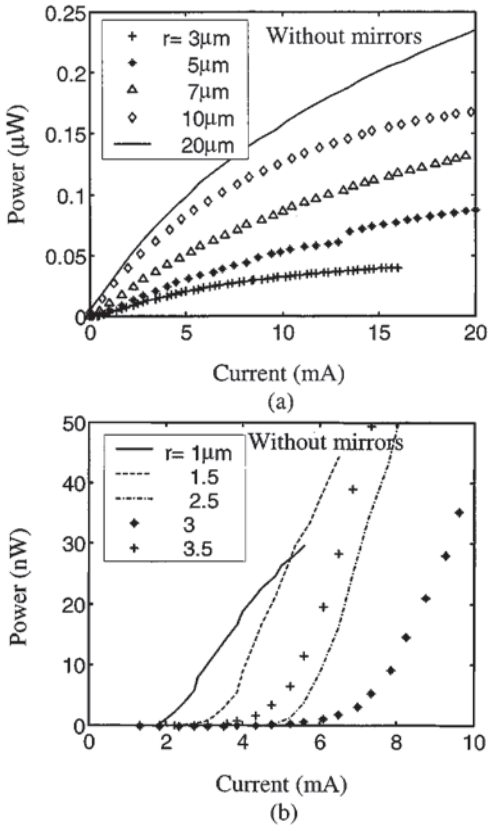

Fig. 4. *L-I* characteristics of LEDs *without* top and bottom mirrors for (a) large aperture sizes and (b) small aperture sizes.

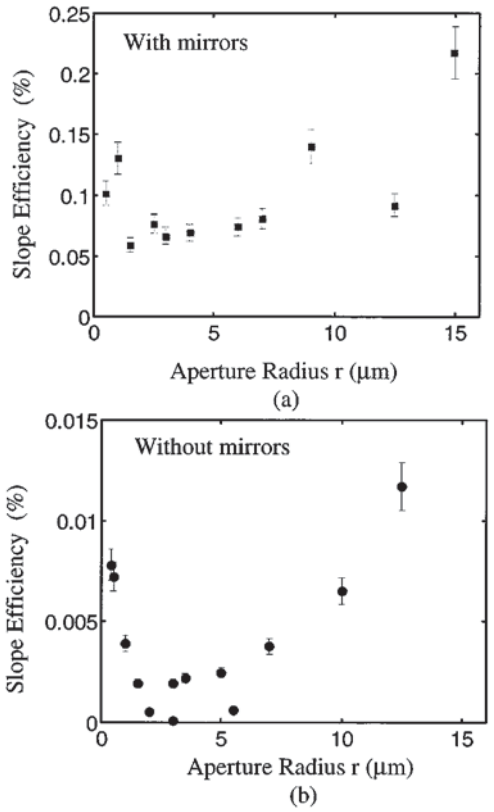

Fig. 5. Measured slope efficiency for devices (a) with and (b) without vertical mirrors. Note that a distinct enhancement in efficiency can be seen for device aperture sizes less than 2 μm.

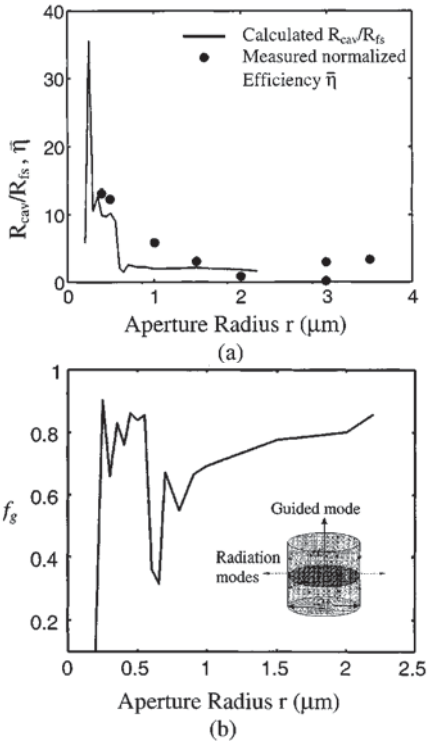

Fig. 6. (a) Measured efficiency and calculated spontaneous emission rate enhancement in mirror-free cylindrical microcavities. (b) Calculated fraction of photons emitted into the guided modes of the cavity when the cavity radius approaches the photon wavelength in the material, with inset showing the schematic and modes of a cylindrical microcavity described in the text.

results of Fig. 6. The important aspect to note here is that the enhancement in the spontaneous emission is observed even in devices without mirrors in the vertical direction. Therefore, it appears that lateral confinement is sufficient for realizing microcavity LEDs. Of course, higher power is attainable with the incorporation of mirrors.

The spontaneous emission rate, in terms of the joint electronic density of states, is [14]

$$R_{\rm sp} = \frac{2\pi}{\hbar} \sum_{{\rm mod}\,es} \frac{e^2}{m_0^2 \omega_{{\rm mod}\,e}^2} \left| M_{cv}^{{\rm mod}\,e} \right|^2 V \times \left(\frac{\rho(\kappa)}{dE_{eh}/d\kappa} \right)_{E_{eh}=\hbar\omega_{{\rm mod}\,e}} \times f_e(E_c) f_h(E_v) \quad (1)$$

where

ω	photon frequency at different modes;
$M_{cv}^{{\rm mod}\,e}$	matrix element;
V	volume of the active region;
$\rho(\kappa)$	mode density;
κ	wave vector,
E_{eh}	photon energy;
f_e, f_h	electron and hole occupation function, respectively;
E_c, E_v	energies in the conduction and valence bands, respectively.

The quasi-Fermi levels in the conduction and valence bands are adjusted so that the electron and hole densities in the intrinsic active region are equal. The spontaneous emission rate in a cavity can be found by converting the sum over the photon states into a

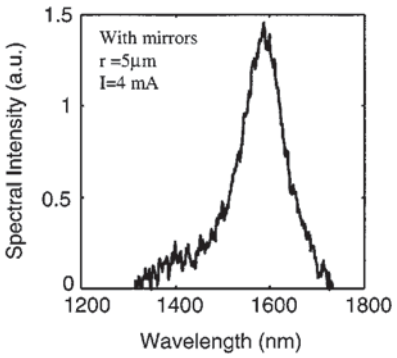

Fig. 7. Measured electroluminescent spectrum for a 5 μm radius microcavity LED with vertical Ag and DBR mirrors at bias current of 4 mA.

frequency integral using the 3-D density of states multiplied by factors of 2 for degenerate linear polarizations of a plane wave mode and one third for the average over zone center Bloch functions [33].

The calculations were performed for our DBR-free cylindrical cavities (InGaAs/InGaAsP/InP, $n = 3.6$) confined laterally by oxide dielectric (Al_xO_y, $n = 1.6$) for aperture radii ranging from 0.2 to 2.2 μm. The results for the ratio of the spontaneous emission rate in the cavity to that without a cavity and with the same active area ($R_{\rm cav}/R_{\rm fs}$) as a function of the radius is shown in Fig. 6(a) for an injected carrier density of $n = 10^{17}$ cm^{-3}, along with the measured efficiency for the cylindrical microcavities without vertical mirrors. The trend of the measured efficiency enhancement agrees well with the calculated spontaneous emission enhancement $R_{\rm cav}/R_{\rm fs}$. It is apparent that for large cavities the spontaneous emission rate tends to the free-space rate. When the cavity radius r becomes comparable to the peak wavelength of the light divided by the refractive index of the core (λ/n), a considerable enhancement in $R_{\rm cav}/R_{\rm fs}$ (Fig. 6(a)) and the fraction of photons emitted into the guided modes of the cavity f_g is observed (Fig. 6(b)).

The spectral output of the devices was measured and representative data are shown in Fig. 7 for a device with top and bottom mirrors and having an aperture radius of 5 μm. The emission peak is observed at 1.6 μm. The emission spectrum of the devices with top and bottom mirrors has a smaller linewidth (FWHM) than that of the devices without mirrors. The linewidth decreases from 60 meV for the mirror-less devices to 33 meV for the devices with 3-D confinement, which represents a reduction of 45%. It may be remembered that the active region material in our device is bulk $In_{0.53}Ga_{0.47}As$, for which the spontaneous emission linewidth at 300 K is 50–60 meV. Even broader linewidths, of the order of 90 meV, have been measured in large area InGaAsP LEDs [10]. The narrowing of the linewidth observed in the MCLEDs is related to the cavity Q in the vertical direction and further narrowing should be attainable by increasing the cavity finesse.

B. Far-Field Radiation Pattern

The far-field radiation pattern of devices with aperture diameters ranging from 1 to 30 μm and with or without mirrors was measured by using a pinhole apertured Ge detector to collect the light intensity at different spatial positions. The collected light

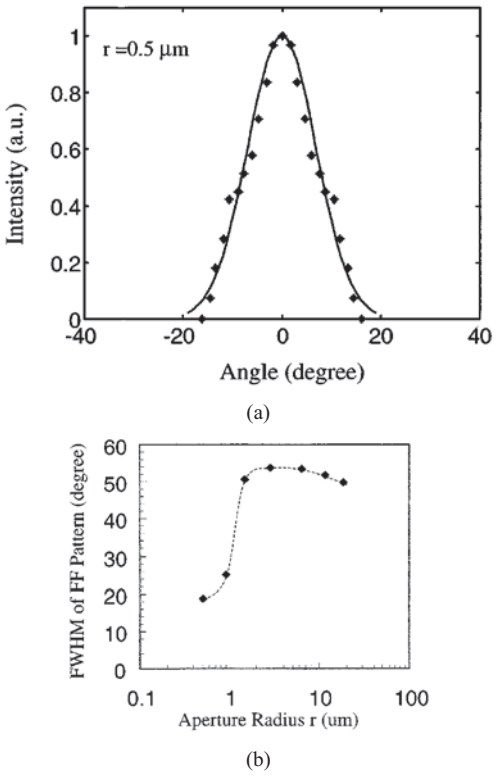

Fig. 8. (a) Measured far-field radiation pattern of 0.5-μm aperture mirror-free microcavity LED. (b) Linewidth (FWHM) of far-field radiation pattern for LEDs, without mirrors, as a function of lateral aperture size.

intensity is then normalized to obtain a spatial distribution of the output at far field. For devices with aperture sizes ranging from 3 to 30 μm, the angular width (FWHM) of the pattern is $\sim 50°$. Smaller devices, with aperture diameter equal to 1 μm, exhibit patterns with an angular width of 20°. The data are shown in Fig. 8. In fact, the decrease in the FWHM is noticeable once the aperture size is reduced to less than 2 μm. This is in reasonable agreement with the observed trend of the slope efficiency. Nonetheless, it should be noted that the observed onset of microcavity effect is for an aperture size which is still three times λ/n. This is in agreement with other reported data on GaAs-based microcavity light sources [25].

While it is very unlikely that the 1-μm device has only a single mode, nonetheless, the increase in directionality of the output indicates that there are, at best, a few modes and true microcavity effects are operative. It has been shown by Vurgaftman [14] and Schubert [15] that when the lateral cavity dimension, or aperture size, approaches λ/n, the output beam is vertically collimated with an intensity peak close to the origin. The considerable narrowing from 50° to 20 ° in the FWHM of the far-field pattern measured for the 1-μm diameter MCLEDs is in agreement with theoretical predictions.

C. Small-Signal Modulation Bandwidth

Room temperature modulation response of the MCLEDs was measured by using a HP8510 network analyzer. The devices are driven with -10 dBm RF modulation power, superimposed through a bias-T on a dc bias through a 100-GHz microwave probe. The output light is collected by a cleaved fiber, amplified, and detected by a high-speed photoreceiver. This detected

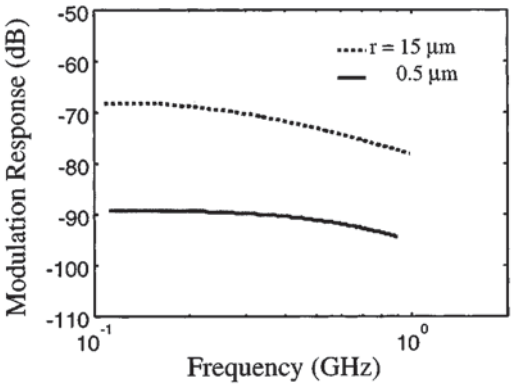

(a)

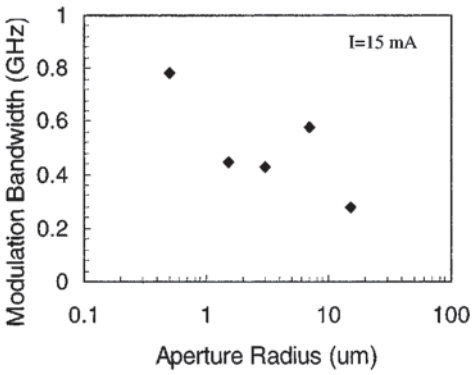

(b)

Fig. 9. (a) Average (fitted) measured small-signal modulation response of microcavity LEDs with vertical mirrors. (b) Variation of measured modulation bandwidth with device (aperture) size.

signal is fed to the network analyzer. It was observed (Fig. 9) that while the 3-dB bandwidth of the larger devices varies between 0.4–0.5 GHz, the measured bandwidth of the 1-μm device is 0.8 GHz, which represents an enhancement by a factor of 1.6. It was estimated that the bandwidth limited by extrinsic factors (diode capacitance, series resistance and other parasitic circuit elements) is at least 20 GHz for our high-speed ground-signal-ground (GSG) contact configuration, which is much larger than the measured bandwidths. We, therefore, believe that the measured values reflect intrinsic device properties. The bandwidths of 0.5 and 0.8 GHz translate to recombination lifetimes of 2 and 1.25 ns, respectively. It is interesting to note that an enhancement of the spontaneous emission rate by a factor of 5 and 2.3 in quantum dot microcavities has been reported by Gerald [17] and Graham [34], respectively. It is important to consider the role of nonradiative recombination at the oxide-semiconductor interface and surface of the device, as the device size becomes smaller. This may account for a decrease in the recombination lifetime. However, the fact that the output power remains almost constant, in spite of a decrease in device size, and the observed directionality in output and enhancement of slope efficiency lead us to believe that the enhancement in modulation bandwidth is a true microcavity effect.

IV. Conclusion

When the recombination volume of light-emitting diodes is shrunk to the order of the wavelength λ, then the photon density of states is modified and there are one or few photon modes supported by the cavity. All the photons generated by recombination, or otherwise, are in these few modes. Such modal characteristics give rise to spatial coherence and a directional output. Furthermore, since the spontaneous emission rate can be enhanced, the modulation bandwidth is increased. All these attributes make microcavity LEDs very attractive sources for fiber communication. We report here on the properties of 1.6-μm microcavity LEDs with lateral confinement provided by the oxidation of double $In_{0.52}Al_{0.48}As$ layers.

The devices are made with InP-based heterostructures and consist of a InGaAs recombination region buried in InGaAsP spacers. Two types of MCLEDs have been tested, with and without mirrors in the vertical (output) direction. The cavity Q in the vertical direction for the device with mirrors is estimated to be $\sim$35–45. Devices with oxide-confined aperture sizes in the range of 1–30 μm (diameter) have been tested. True microcavity effects have been observed in the smallest devices (1 μm) irrespective of the presence of the mirrors. Thus, a more directional far-field pattern (FWHM $\sim 20^\circ$), enhancement of the output slope efficiency and an increase in the small-signal modualtion bandwidth by a factor of 1.6, have all been measured. The maximum power output of the devices is measured to be $\sim$30 μW. Our results indicate that useful MCLEDs can be realized with only lateral confinement to $r \sim \lambda/n$.

Acknowledgment

The authors thank Prof. J. Singh and Dr. I. Vurgaftman for useful discussions and help with the calculations. They also acknowledge the discussions with Dr. H. Gebretsadik and B. Kochman.

References

[1] C. Wilmsen, H. Temkin, and L. A. Coldren, Eds., *Vertical-Cavity Surface-Emitting Lasers: Design, Fabrication, Characterization, and Applications*. Cambridge, U.K.: Cambridge Univ. Press, 1999.

[2] T. Baba, Y. Yogo, K. Suzuki, F. Koyama, and K. Iga, "Near room temperature continuous wave lasing characteristics of GaInAsP/InP surface emitting laser," *Electron. Lett.*, vol. 29, pp. 913–915, 1993.

[3] J. Dudley, D. I. Babic, R. Mirin, L. Yang, B. I. Miller, R. J. Ram, T. Reynolds, E. L. Lu, and J. E. Bowers, "Low threshold wafer-fused long wavelength vertical cavity lasers," *Appl. Phys. Lett.*, vol. 64, pp. 1463–1465, 1994.

[4] N. M. Margalit, J. Piprek, S. Zhang, D. I. Babic, K. Streubel, R. P. Mirin, J. R. Wesslmann, J. E. Bowers, and E. L. Hu, "64°C continuous-wave operation of a 1.54 μm vertical-cavity lasers," *IEEE J. Select. Topics Quantum Electron.*, vol. 3, pp. 359–365, 1997.

[5] H. Yokoyama, "Physics and device applications of optical microcavities," *Science*, vol. 256, pp. 66–70, 1992.

[6] E. F. Schubert, N. E. J. Hunt, M. Micovic, R. J. Malik, D. L. Sivco, A. Y. Cho, and G. J. Zydzik, "Highly efficient light-emitting diodes with microcavities," *Science*, vol. 265, pp. 943–945, 1994.

[7] H. De Neve, J. Blondelle, R. Baets, P. Demeester, P. Van Daele, and G. Borghs, "Resonant cavity LED's," in *Microcavities and Photonic Bandgaps*, J. Rarity and C. Weisbuch, Eds. Norwell, PA: Kluwer, 1996, pp. 333–342.

[8] H. Benisty, J. Gerard, R. Hondre, J. Rarity, and C. Weisbuch, Eds., *Confined Photon Systems: Fundamentals and Applications*. New York: Springer-Verlag, 1999.

[9] T. Baba, "Photonic crystals and microdisk cavities based on GaInAsP-InP system," *IEEE J. Select. Topics Quantum Electron.*, vol. 3, pp. 808–830, Mar. 1997.

[10] E. F. Schubert, Y.-H. Wang, A. Y. Cho, L.-W. Tu, and G. J. Zydzik, "Resonant cavity light-emitting diode," *Appl. Phys. Lett.*, vol. 60, pp. 921–923, 1992.

[11] N. E. J. Hunt, E. F. Schubert, R. F. Kopf, D. L. Silvco, A. Y. Cho, and G. J. Zydzik, "Increased fiber communications bandwidth from a resonant cavity light emitting diode emitting at $\lambda = 940$ nm," *Appl. Phys. Lett.*, vol. 63, pp. 2600–2602, 1993.

[12] D. L. Huffaker, C. C. Lin, J. Shin, and D. G. Deppe, "Resonant cavity light emitting diode with an Al_xO_y/GaAs reflector," *Appl. Phys. Lett.*, vol. 66, no. 23, pp. 3096–3098, 1995.

[13] H. De Neve, J. Blondelle, R. Baets, P. Demeester, P. Van Daele, and G. Borghs, "High efficiency planar microcavity LED's comparison of design and experiment," *IEEE Photon. Technol. Lett.*, vol. 7, pp. 287–289, 1995.

[14] I. Vurgaftman and J. Singh, "Spatial and spectral characteristics of spontaneous emission from semiconductor quantum wells in microscopic cylindrical cavities," *Appl. Phys. Lett.*, vol. 67, pp. 3865–3867, 1995.

[15] E. F. Schubert and N. E. J. Hunt, "Enhancement of spontaneous emission in microcavities," in *Vertical-Cavity Surface-Emitting Lasers: Design, Fabrication, Characterization, and Applications*, 1999, pp. 68–107.

[16] H. Benisty, H. DeNeve, and C. Weisbuch, "Impact of planar microcavity effects on light extraction," *IEEE J. Quantum Electron.*, vol. 34, pp. 1612–1642, 1998.

[17] J. Gerard, B. Sermage, B. Gayral, B. Legrand, E. Costard, and V. Thierry-Mieg, "Enhanced spontaneous emission by quantum boxes in a monolithic optical microcavity," *Phys. Rev. Lett.*, vol. 81, no. 5, pp. 1110–1113, 1998.

[18] N. E. J. Hunt, E. F. Schubert, R. A. Logan, and G. J. Zydzik, "Enhanced spectral power density and reduced linewidth at 1.3 μm in an InGaAsP quantum well resonant cavity light-emitting diode," *Appl. Phys. Lett.*, vol. 61, pp. 2287–2289, 1992.

[19] M. Jalonen, J. Kongas, M. Toivonen, P. Savolainen, S. Orsila, A. Salokatve, and M. Pessa, "Monolithic 1.3 μm resonant cavity light emitting diode grown by solid source molecular beam epitaxy," *Electron. Lett.*, vol. 34, pp. 1519–1520, 1998.

[20] P. Landais, B. Roycroft, A. Shaw, B. Depreter, I. Moerman, and J. Hegarty, "Small-signal analysis of 1.3-μm microcavity light-emitting diodes," *IEEE Photon. Technol. Lett.*, vol. 11, pp. 1342–1344, Nov. 1999.

[21] D. L. Huffaker, D. G. Deppe, K. Kumar, and T. J. Rogers, "Native-oxide defined buried ring contact for low threshold vertical-cavity lasers," *Appl. Phys. Lett.*, vol. 65, pp. 97–99, 1995.

[22] G. M. Yang, M. H. MacDougal, and P. D. Dapkus, "Ultralow threshold current vertical-cavity surface-emitting lasers obtained with selective oxidation," *Electron. Lett.*, vol. 31, pp. 886–888, 1995.

[23] K. L. Lear, K. D. Choquete, R. P. Schneider Jr., S. P. Kilcoyne, and K. M. Geib, "Selectively oxidized vertical-caivity surface-emitting lasers with 50% power conversion efficiency," *Electron. Lett.*, vol. 31, pp. 208–209, 1995.

[24] B. J. Thibeault, E. R. Hegblom, Y. A. Akulova, J. Ko, R. Naone, and L. A. Coldren, "Electrical and optical losses in dielectrically apertured vertical cavity lasers," *SPIE*, vol. 3003, pp. 86–99, 1997.

[25] D. Huffaker and D. G. Deppe, "Spontaneous coupling to planar and index-confined quasimodes Fabry-Perot microcavities," *Appl. Phys. Lett.*, vol. 67, pp. 2594–2596, 1995.

[26] H. Gebretsadik, K. Kamath, W. D. Zhou, P. K. Bhattacharya, C. Caneau, and R. Bhat, "Lateral oxidation of InAlAs in InP-based heterostructures for long wavelength vertical cavity surface emitting laser applications," *Appl. Phys. Lett.*, vol. 72, pp. 135–137, 1998.

[27] H. Gebretsadik, P. K. Bhattacharya, K. Kamath, O. R. Qasaimeh, D. J. Klotzkin, C. Caneau, and R. Bhat, "InP-based 1.5 μm vertical cavity surface emitting laser with epitaxially grown defect-free GaAs-based distributed Bragg reflectors," *Electron. Lett.*, vol. 34, pp. 1316–1317, 1998.

[28] S. J. Caracci, M. R. Krames, N. Holonyk Jr., M. J. Ludowise, and A. Fischer-Colbrie, "Long wavelength ($\lambda \sim 1.5$ μm) native-oxide-defined InAlAs-AnP-InGaAsP quantum well heterostructure laser diodes," *J. Appl. Phys.*, vol. 75, pp. 2706–2708, 1994.

[29] O. Blum, K. M. Geib, M. J. Hafich, J. F. Klen, and C. I. H. Ashby, "Wet thermal oxidation of AlAsSb lattice matched to InP for optoelectronic applications," *Appl. Phys. Lett.*, vol. 68, pp. 3129–3131, 1996.

[30] P. Legay, F. Caillet, J. Decobert, L. Leprince, G. Le Roux, and M. Quillec, "Oxide confining layer on an InP substrate," *J. Appl. Phys.*, vol. 85, pp. 2428–2430, 1999.

[31] H. Gebretsadik, K. Zhang, K. Kamath, X. Zhang, and P. Bhattacharya, "Recombination characteristics of minority carriers near the Al_xO_y/GaAs interface using the light beam induced current technique," *Appl. Phys. Lett.*, vol. 71, no. 26, pp. 3865–3867, 1997.

[32] D. Biswas, P. R. Berger, U. Das, J. E. Oh, and P. K. Bhattacharya, "Investigation of the interface region produced by molecular beam epitaxial regrowth," *J. Electron. Mat.*, vol. 18, no. 2, pp. 137–142, 1989.

[33] J. Singh, *Physics of Semiconductors and Their Heterostructures*. New York: McGraw-Hill, 1993.

[34] L. Graham, D. Huffaker, and D. Deppe, "Spontaneous lifetime control in a native-oxide-apertured microcavity," *Appl. Phys. Lett.*, vol. 74, no. 17, pp. 2408–2410, 1999.

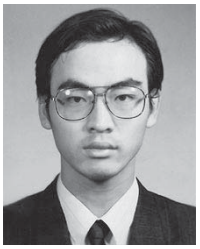

Weidong Zhou (S'99) received the B.E. and M.E. degrees in electrical engineering from Tsinghua University, China, in 1993 and 1996, respectively. He is currently working toward the Ph.D. degree in electrical engineering at the University of Michigan, Ann Arbor.

His research area include optoelectronic device design, fabrication, characterization, and OEIC circuits design.

Mr. Zhou is a member of Tau Beta Pi.

Pallab Bhattacharya (M'78–SM'83–F'89) received the Ph.D. degree from the University of Sheffield, Sheffield, U.K., in 1978.

He is currently the James R. Mellor Professor of Engineering in the Department of Electrical and Engineering and Computer Science at the University of Michigan, Ann Arbor. His teaching and research interests include liquid-phase and molecular beam epitaxy of elemental and III–V compound semiconductors, materials characterization, electronic and optoelectronic devices, and optoelectronic integrated circuits. He was on the faculty of Oregon State University, Corvallis, from 1978 to 1983, and since 1983, he has been with the University of Michigan. He was an Invited Professor at the Ecole Polytechnique Federale de Lausanne, Switzerland, from 1981 to 1982. He has published over 300 technical articles in archival journals. He is author of the textbook *Semiconductor Optoelectronic Devices* (Englewood Cliffs, NJ: Prentice-Hall, 1994, 1st ed., and 1997 2nd ed.).

Dr. Bhattacharya is an Editor of the IEEE TRANSACTIONS ON ELECTRON DEVICES and has edited *Properties of Lattice-Matched and Strained InGaAs* (U.K.: INSPEC, 1993) and *Properties of III–V Quantum Wells and Superlattices* (U.K.: INSPEC, 1996). He has served on the Advisory Board of the Electrical and Communications Systems Division at the National Science Foundation. He has also served on several other committees and panels in academia, government, industry, and technical conferences. He has received the Parker Rhodes Scholarship from the University of Sheffield, the Research Excellence Award from the University of Michigan, the Alexander von Humboldt Award, the SPIE Technology Achievement Award, the John Simon Guggenheim Award, IEEE (LEOS) Distinguished Lecturer Award, and the S. S. Attwood Award from the University of Michigan. He is a member of the American Physical Society and a fellow of the Optical Society of America.

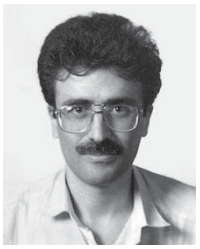

Omar Qasaimeh received the B.S. and M.S. degrees in electrical engineering from Jordan University of Science and Technology, Irbid, Jordan, in 1992 and 1994, respectively. He is currently working toward the Ph.D. degree at the University of Michigan, Ann Arbor.

His research interests include fabrication, characterization, and modeling of high-speed optoelectronic devices and integrated circuits.